Articles

NiO/La_2O_3-ZrO_2/WO_3 Catalyst Prepared by Doping ZrO_2 with La_2O_3 and Modifying with WO_3 for Acid Catalysis

Jong Rack Sohn,* Hee Dong Choi, and Dong Cheol Shin

Department of Applied Chemistry, Engineering College, Kyungpook National University, Daegu 702-701, Korea
**E-mail: jrsohn@knu.ac.kr*
Received January 18, 2006

A series of catalysts, NiO/La_2O_3-ZrO_2/WO_3, for acid catalysis was prepared by the precipitation and impregnation methods. For the NiO/La_2O_3-ZrO_2/WO_3 samples, no diffraction lines of nickel oxide were observed, indicating good dispersion of nickel oxide on the catalyst surface. The catalyst was amorphous to X-ray diffraction up to 300 °C of calcination temperature, but the tetragonal phase of ZrO_2 and monoclinic phase of WO_3 by the calcination temperatures from 400 °C to 700 °C were observed. The role of La_2O_3 in the catalyst was to form a thermally stable solid solution with zirconia and consequently to give high surface area and acidity. The high acid strength and high acidity were responsible for the W=O bond nature of complex formed by the modification of ZrO_2 with WO_3. For 2-propanol dehydration the catalyst calcined at 400 °C exhibited the highest catalytic activity, while for cumene dealkylation the catalyst calcined at 600 °C showed the highest catalytic activity. 25-NiO/5-La_2O_3-ZrO_2/15-WO_3 exhibited maximum catalytic activities for two reactions due to the effects of WO_3 modifying and La_2O_3 doping.

Key Words : NiO/La_2O_3-ZrO_2/WO_3 catalysts, Doping with La_2O_3, Modification with WO_3, 2-Propanol dehydration, Cumene dealkylation

Introduction

Many kinds of solid acids have been found: their acidic properties, their catalysis, and the structure of acid site have been elucidated and those results have been reviewed by several workers.[1-4] Acid catalysis plays a key role in many important reactions of the chemical and petroleum industries, and in environmentally benign chemical processes.[2,5] Liquid superacids based on HF, which are efficient and selective at room temperature,[6] are not suitable for industrial processes due to separation problems tied with environmental protection. Conventional industrial acid catalysts, such as sulfuric acid, $AlCl_3$, and BF_3, have unavoidable drawbacks because of their severe corrosivity and high susceptibility to water. The search for environmentally benign heterogeneous catalysts has driven the worldwide research of new materials as substitutes for current liquid acids and halogen-based solid acids.[2,3] Among them sulfated oxides, such as sulfated zirconia, titania, and iron oxide exhibiting high thermostability, superacidic property, and high catalytic activity, have evoked increasing interest.[2,3] The strong acidity of zirconia-supported sulfate has attracted much attention because of its ability to catalyze many reactions such as cracking, alkylation, and isomerization. The potential for a heterogeneous catalyst has yielded many papers on the catalytic activity of sulfated zirconia materials.[3,7-10] Sulfated zirconia incorporating Fe and Mn has been shown to be highly active for butane isomerization, catalyzing the reaction even at room temperature.[11,12] The promotion in activity of catalyst has been confirmed by several other research groups.[13-15] Coelho *et al.* have discovered that the addition of Ni to sulfated zirconia causes an activity enhancement comparable to that caused the addition of Fe and Mn.[16]

It has been reported by several workers that the addition of platinum to zirconia modified by sulfate ions enhances catalytic activity in the skeletal isomerization of alkanes without deactivation, when the reaction is carried out in the presence of hydrogen.[17-19] The high catalytic activity and small deactivation can be explained by the elimination of the coke by hydrogenation and hydrogenolysis,[17] and by the formation of Brönsted acid sites from H_2 on the catalysts.[18] Recently, Hino and Arata have reported zirconia-supported tungsten oxide as an alternative material in reaction requiring strong acid sites.[3,20] The several advantages of tungstate over sulfate as dopant include the facts that it does not suffer from dopant loss during thermal treatment and that it undergoes significantly less deactivation during catalytic reaction.[21] It was also reported that a small amount of rare-earth elements in zirconia powder can stabilize the tetragonal and cubic phase over a wide range of temperature.[22]

In this paper, we report NiO supported on ZrO_2 catalyst prepared by doping ZrO_2 with La_2O_3 and modified with WO_3 to improve catalytic activity for acid catalysis and thermal stability. The characterization of the samples was performed by means of IR, X-ray diffraction (XRD), differential scanning calorimetry (DSC), and surface area mea-

surements. For the acid catalysis, the 2-propanol dehydration and cumene dealkylation were used as test reactions.

Experimental Section

Catalysts. The La_2O_3-ZrO_2 mixed oxide was prepared by a coprecipitation method using an aqueous ammonia as the precipitation reagent. The coprecipitate of $La(OH)_3$-$Zr(OH)_4$ was obtained by adding aqueous ammonia slowly into a mixed aqueous solution of lanthanium nitrate and zirconium oxychloride [Junsei Chemical Co.] at 25 °C with stirring until the pH of mother liquor reached about 8. NiO/La_2O_3-ZrO_2 was prepared by adding aqueous ammonia slowly into a mixed solution of $NiCl_2$ solution and La_2O_3-ZrO_2 with stirring until the pH of solution reached about 8.

The catalysts containing various tungsten oxide contents were prepared by adding an aqueous solution of ammonium metatungstate[$(NH_4)_6(H_2W_{12}O_{40})$-$nH_2O$] to the NiO/$La_2O_3$-$ZrO_2$ powder followed by drying and calcining at high temperatures for 1.5 h in air. This series of catalysts are denoted by their weight percentage of NiO and WO_3. For example, 25-NiO/5-La_2O_3-ZrO_2/15-WO_3 indicates the catalyst containing 25 wt% NiO, and 15 wt% WO_3, and 5 mol% La_2O_3 regarding only ZrO_2.

Procedure. 2-Propanol dehydration was carried out at 160 and 180 °C in a pulse microreactor connected to a gas chromatograph. Fresh catalyst in the reactor made of 1/4 in. stainless steel was pretreated at 400 °C for 1 h in the nitrogen atmosphere. Pulses of 1 μL 2-propanol were injected into a N_2 gas stream which passed over 0.05 g of catalyst. Packing material for the gas chromatograph was diethyleneglycol succinate on Shimalite and column temperature was 150 °C. Catalytic activity for 2-propanol dehydration was represented as the mol of propylene converted per gram of catalyst.

Cumene dealkylation was carried out at 400-450 °C in the same reactor as above. Packing material for the gas chromatograph was Benton 34 on chromosorb W and column temperature was 130 °C. Catalytic activity for cumene dealkylation was represented as the mol of benzene converted from cumene per gram of catalyst. Conversion for both reactions was taken as the average of the first to sixth pulse values.

Chemisorption of ammonia was employed as a measure of acid amount of catalysts. The amount of chemisorption was obtained as the irreversible adsorption of ammonia.[23-25] The specific surface area was determined by applying the BET method to the adsorption of nitrogen at −196 °C.

FTIR spectra were obtained in a heatable gas cell at room temperature using a Mattson Model GL6030E spectrometer. Self-supporting catalyst wafers contained about 9 mg/cm^2. Prior to obtaining the spectra, the samples were heated under vacuum at 500 °C for 1 h.

X-ray photoelectron spectra was obtained with a VG scientific model ESCALAB MK-11 spectrometer. Al K_α and Mg K_α were used as the excitation source, usually at 12 kV and 20 mA. The analysis chamber was at 10^{-9} torr or better and the spectra of sample, as fine powder, were analyzed. Binding energies were referenced to the C_{1s} level of the adventitious carbon at 285.0 eV

Catalysts were checked in order to determine the structure of the support as well as that of tungsten oxide by means of a Jeol Model JDX-8030 diffractometer, employing Cu Kα (Ni-filtered) radiation.

DSC measurements were performed in air by a PL-STA model 1500H apparatus, and a heating rate was 5 °C per min. For each experiment 10-15 mg of the sample was used.

Results and Discussion

Crystalline Structures of NiO/La_2O_3-ZrO_2/WO_3. The crystalline structures of 25-NiO/5-La_2O_3-ZrO_2/15-WO_3 calcined in air at different temperatures for 1.5 h were examined. As shown in Figure 1, the catalyst was amorphous to X-ray diffraction up to 300 °C. However, for the calcination temperature of 400 °C XRD data indicated a two-phase mixture of monoclinic phase of WO_3 and tetragonal phase of ZrO_2. The amount of two phases of ZrO_2 and WO_3 increased with increasing calcination temperature, indicating that the interaction between NiO or WO_3 and ZrO_2 hinders the transition of ZrO_2 from amorphous to tetragonal phase.[26,27] The presence of NiO and WO_3 strongly influences the development of textural properties with temperature in comparison with pure ZrO_2. In fact, it is reported that for pure ZrO_2 two phases of tetragonal and monoclinic ZrO_2 are present at the calcination temperature of 350 °C because of no interaction of zirconia.[28] No phase of NiO was observed in any phase at all calcination temperature, indicating good dispersion of NiO on the surface of ZrO_2 support due to the interaction between them.

The XRD patterns of 25-NiO/5-La_2O_3-ZrO_2/WO_3 calcin-

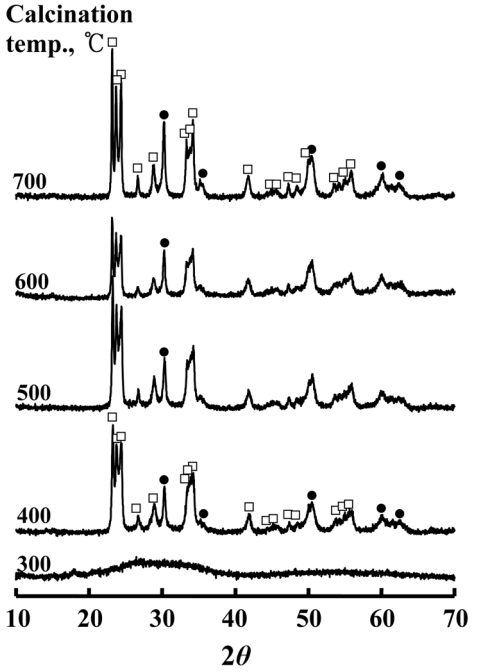

Figure 1. X-ray diffraction patterns of 25-NiO/5-La_2O_3-ZrO_2/15-WO_3 calcined at different temperatures for 1.5 h: ● , tetragonal phase of ZrO_2; □ , monoclinic phase of WO_3.

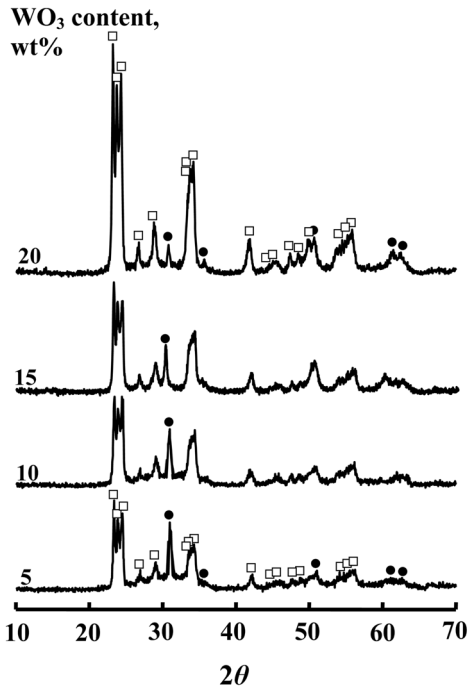

Figure 2. X-ray diffraction patterns of 25-NiO/5-La$_2$O$_3$-ZrO$_2$/WO$_3$ having different WO$_3$ contents at 400 °C for 1.5 h: ● , tetragonal phase of ZrO$_2$; □ , monoclinic phase of WO$_3$.

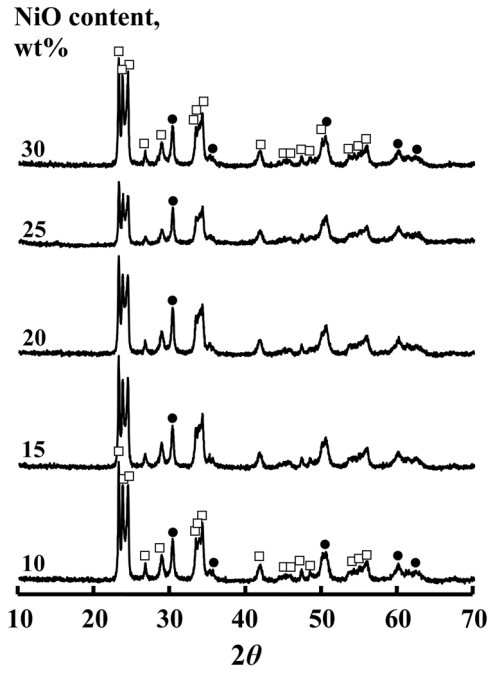

Figure 3. X-ray diffraction patterns of NiO/5-La$_2$O$_3$-ZrO$_2$/15-WO$_3$ having different NiO contents at 400 °C for 1.5 h: ● , tetragonal phase of ZrO$_2$; □ , monoclinic phase of WO$_3$.

ed at 400 °C for 1.5 h as a function of WO$_3$ content are shown in Figure 2. The XRD data indicated the presence of a two-phase mixture of monoclinic phase of WO$_3$ and tetragonal phase of ZrO$_2$. In general, for the calcination temperature of 400-500 °C the hexagonal and monoclinic phases of WO$_3$ are present.[29] However, in case of NiO-

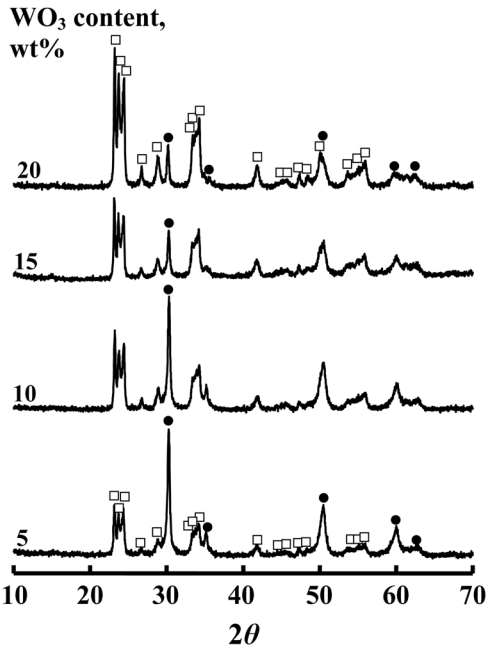

Figure 4. X-ray diffraction patterns of 25-NiO/5-La$_2$O$_3$-ZrO$_2$/WO$_3$ having different WO$_3$ contents at 600 °C for 1.5 h: ● , tetragonal phase of ZrO$_2$; □ , monoclinic phase of WO$_3$.

La$_2$O$_3$-ZrO$_2$/WO$_3$ only the monoclinic phase of WO$_3$ was observed, as shown in Figures 1 and 2.

XRD patterns of NiO/5-La$_2$O$_3$-ZrO$_2$/15-WO$_3$ calcined at 400 °C for 1.5 h as a function of NiO content are shown in Figure 3. NiO was amorphous to X-ray diffraction regardless of NiO content up to 30 wt% NiO, indicating excellent dispersion on the surface of catalyst. However, the other components, WO$_3$ and ZrO$_2$ except NiO were observed as crystalline forms at 5 wt% WO$_3$ and above. Namely, monoclinic phase of WO$_3$ and tetragonal phase of ZrO$_2$ were appeared in the range of 15-30 wt% NiO. Also, in the case of 30-NiO/5-La$_2$O$_3$-ZrO$_2$/15-WO$_3$ containing high NiO content there is a possibility that lanthanum nickel oxide from NiO and La$_2$O$_3$ at calcination temperature is formed and consequently crystalline NiO phase due to the decreased amount of NiO is not observed on X-ray diffraction patterns.

The XRD patterns of the 25-NiO/5-La$_2$O$_3$-ZrO$_2$/WO$_3$ catalysts calcined at 600 °C for 1.5 h as a function of WO$_3$ content are shown in Figure 4. Similarly to the 25-NiO/5-La$_2$O$_3$-ZrO$_2$/WO$_3$ samples calcined at 400 °C, in the case of samples calcined at 600 the monoclinic phase of WO$_3$ was observed and the amount increased with increasing WO$_3$ content. For the ZrO$_2$ only tetragonal phase of ZrO$_2$ was observed and the amount decreased with increasing WO$_3$ content because of the decrease of relative amount of ZrO$_2$ regarding all components.

X-ray Photoelectron Spectra and Infrared Spectra. Interactions with a support can dramatically change the properties metals or metal oxides.[30] We examined the W (4f) spectra of some 25-NiO/5-La$_2$O$_3$-ZrO$_2$/WO$_3$ samples containing different tungsten oxide contents and calcined at 500 °C. The W 4f$_{7/2}$ binding energy measured for 25-NiO/

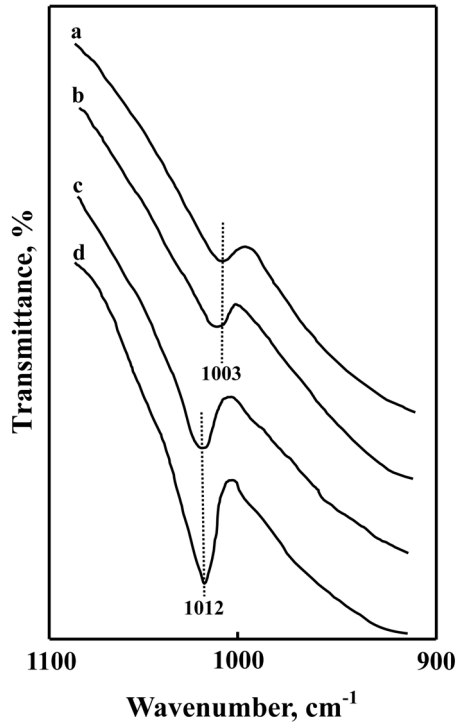

Figure 5. Infrared spectra of 25-NiO/5-La_2O_3-ZrO_2/15-WO_3 evacuated at different temperatures: (a) 100 °C, (b) 200 °C, (c) 300 °C, and 500 °C.

5-La_2O_3-ZrO_2/WO_3 samples occurred at 36 eV and corresponds to tungsten in the +6 oxidation state (WO_3)[31] (This spectra are not shown here). Generally, the spectrum of supported WO_3 is broader than that of WO_3 due to the interaction between the WO_3 and support. It is known that there is a very strong interaction between WO_3 and Al_2O_3 so that tungsten oxide species is present as W^{+6} after calcination of WO_3/Al_2O_3 sample. For 25-NiO/5-La_2O_3-ZrO_2/WO_3 samples calcined in air tungsten oxide species are present as W^{+6}, indicating the strong interaction between WO_3 and La_2O_3-ZrO_2.

To examine the structure of tungsten oxide complex under dehydration conditions, infrared spectra of 25-NiO/5-La_2O_3-ZrO_2/15-WO_3 samples were obtained in a heatable gas cell after evacuation at different temperatures for 1h. The in situ infrared spectra in the 900-1000 cm^{-1} region for 25-NiO/5-La_2O_3-ZrO_2/15-WO_3 are presented in Figure 5. The infrared single band at 1003-1012 cm^{-1} is due to the symmetrical W=O stretching mode of the tungsten oxide complex coordinated to the 5-La_2O_3-ZrO_2 surface.[32] As shown in Figure 5, as evacuation temperature increases, the W=O stretching mode shifts upward from 1003 to 1012 cm^{-1}, the band becomes sharper, and the intensity increases. The similar results have been obtained with the other samples. This shows that the dehydration changes the molecular structures and that the two-dimensional tetrahedrally coordinated tungsten oxide species as well as the octahedrally coordinated polytungstate species are converted into the same highly distorted octahedrally coordinated structure as proposed for the WO_3/TiO_2 system by Wachs *et al.*[33] For the other 25-NiO/5-La_2O_3-ZrO_2/WO_3 samples containing different WO_3 contents and evacuated at 500 °C the band intensity at 1012 cm^{-1} increased with increasing the WO_3 content, indicating that the higher the WO_3 content, the more the octahedrally coordinated WO_3 species.

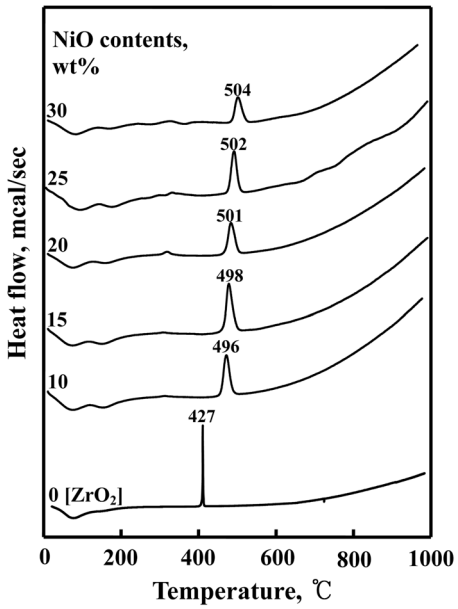

Figure 6. DSC curves of NiO/5-La_2O_3-ZrO_2 precursors having different NiO contents.

Thermal Analysis. In XRD patterns, it was shown that the structure of catalysts was different depending on the calcined temperature. To examine the thermal properties for the precursors of samples more clearly, their thermal analysis has been carried out and the results are illustrated in Figure 6. For pure ZrO_2 the DSC curve showed a broad endothermic peak below 200 °C due to water elimination, and a sharp exothermic peak at 438 °C due to the phase transition of ZrO_2 from amorphous to tetragonal.[34] In the case of NiO/5-La_2O_3-ZrO_2 a broad endothermic peak appeared below 200 °C is also due to the water elimination. However, it is of interest to see the influence of NiO on the crystallization of ZrO_2 from amorphous to tetragonal phase. As shown in Figure 6, the exothermic peak due to the phase transition of ZrO_2 appeared at 427 °C for pure ZrO_2, while for NiO/5-La_2O_3-ZrO_2 it was shifted to higher temperatures, 496-504 °C. Namely, as shown in Figure 6, the higher the content of NiO, the higher the phase transition temperature of ZrO_2. It is considered that the interaction between NiO and ZrO_2 delays the transition of ZrO_2 from amorphous to tetragonal phase.[26,27] No crystalline phase of NiO was observed in XRD patterns due to the interaction between NiO and ZrO_2.

Surface Properties of Catalysts. It is necessary to examine the effect of WO_3, NiO, and La_2O_3 on the surface properties of catalysts, that is, specific surface area, acidity, and acid strength. The specific surface area and acidity of 25-NiO/5-La_2O_3-ZrO_2/WO_3 having different WO_3 contents and calcined at 400 and 600 °C for 1.5 h are listed in Table 1.

Table 1. Specific surface area and acidity of 25-NiO/5-La$_2$O$_3$-ZrO$_2$/WO$_3$ containing different WO$_3$ contents and calcined at 400 and 600 °C for 1.5 h

WO$_3$ content (wt%)	Surface Area (m^2/g)		Acidity (μmol/g)	
	400 °C	600 °C	400 °C	600 °C
5	27	11	46	35
10	35	13	68	42
15	38	31	74	51
20	23	7	45	28

Table 2. Specific surface area and acidity of NiO/5-La$_2$O$_3$-ZrO$_2$/15-WO$_3$ containing different NiO contents and calcined at 400 and 600 °C for 1.5 h

NiO content (wt%)	Surface area (m^2/g)		Acidity (μmol/g)	
	400 °C	600 °C	400 °C	600 °C
10	18	9	35	31
15	22	10	40	38
20	25	17	48	45
25	38	31	74	51
30	21	19	60	38

The presence of tungsten oxide influences the surface area and acidity in comparison with the sample without WO$_3$. The specific surface area and acidity increase gradually with increasing tungsten oxide content up to 15 wt % of WO$_3$. It seems likely that the interaction between tungsten oxide and ZrO$_2$ not only protects catalysts from sintering, but increase the acidity and acid strength due to the double bond nature of the W=O described below.

In addition to tungsten oxide content, we examined the effect of NiO on the surface area and acidity values. The surface area and acidity of NiO/5-La$_2$O$_3$-ZrO$_2$/15-WO$_3$ having different NiO contents and calcined at 400 and 600 °C for 1.5 h are listed in Table 2. Similarly to WO$_3$, NiO also influenced both surface area and acidity values, indicating that the addition of NiO increased gradually both surface area and acidity with increasing NiO content up to 25 wt%. It is known that thermal resistance of zirconia against sintering can be considerably improved by incorporation a second oxide.[35,36]

More active and stable catalyst can be obtained by addition of transition metal, especially noble metals.[37-39] Recently, we reported that the role of Ce in CeO$_2$-ZrO$_2$ catalysts is to form a thermally stable solid solution with ZrO$_2$ and consequently to give high surface area.[40] As listed in Table 3, the addition of La$_2$O$_3$ to ZrO$_2$ also increases both surface area and acidity up to 5 mol% of La$_2$O$_3$. Doping ZrO$_2$ with small amounts of rare-earth elements may tailor its properties for better catalytic performance, to form solid solution.[41] Based on the results of XRD, La$_2$O$_3$ formed a solid solution with ZrO$_2$.

Table 3. Specific surface area and acidity of 25-NiO/La$_2$O$_3$-ZrO$_2$/15-WO$_3$ containing different La$_2$O$_3$ contents and calcined at 400 and 600 °C for 1.5 h

La$_2$O$_3$ content (mol%)	Surface area (m^2/g)		Acidity (μmol/g)	
	400	600	400	600
2.5	21	18	39	27
5	38	31	74	51
10	36	29	59	47
15	28	21	47	35

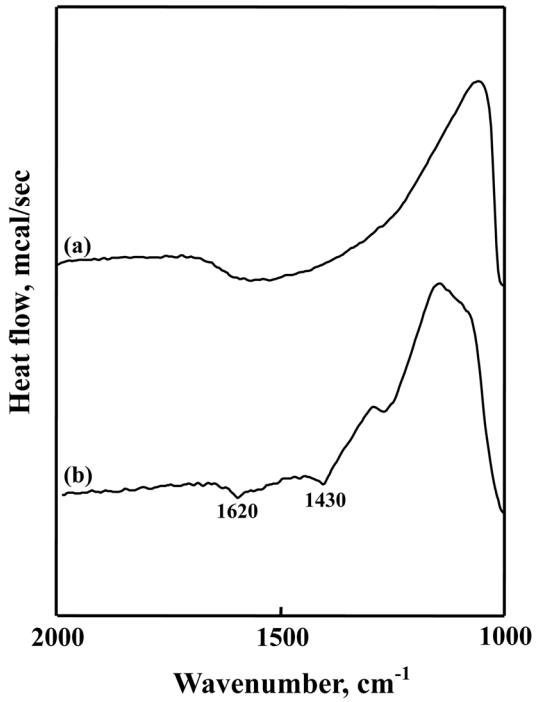

Figure 7. Infrared spectra of NH$_3$ adsorbed on 25-NiO/5-La$_2$O$_3$-ZrO$_2$/15-WO$_3$: (a) background of 25-NiO/5-La$_2$O$_3$-ZrO$_2$/15-WO$_3$ after evacuation at 500 °C for 1 h, (b) NH$_3$ adsorbed on (a), where gas was evacuated at 230 °C for 1 h.

The acid strength of the catalysts was examined by a color change method, using Hammett indicator[25,31] in sulphuryl chloride. 5-NiO/5-La$_2$O$_3$-ZrO$_2$/15-WO$_3$ sample after evacuation at 500 °C for 1 h was estimated to have $H_0 \leq -14.5$, indicating the formation of superacidic sites. Since it was very difficult to observe the color of indicators adsorbed on the catalyst of high nickel oxide content, the low percentage of nickel oxide (5 wt %) was used in this experiment. Acids stronger than $H_0 \leq -11.93$, which corresponds to the acid strength of 100% H$_2$SO$_4$, are superacids.[1-3] Consequently, NiO/La$_2$O$_3$-ZrO$_2$/WO$_3$ catalysts would be solid superacids. The superacidic property is attributed to the double bond nature of the W=O in the complex formed by the interaction of ZrO$_2$ with tungstate, in analogy with the case of ZrO$_2$ modified with chromate and sulfate ion.[35,42,43]

It is well known that infrared spectroscopy of ammonia adsorbed on solid surfaces can distinguish between Brönsted and Lewis acid sites.[44-46] Figure 7 shows the infrared spectra of ammonia adsorbed on 25-NiO/5-La$_2$O$_3$-ZrO$_2$/15-WO$_3$ sample evacuated at 400 °C for 1 h. The band at 1430 cm^{-1} is the characteristic peak of ammonium ion, which is formed on the Brönsted acid sites and the absorption peak at 1620 cm^{-1} is contributed by ammonia coordinately bonded to

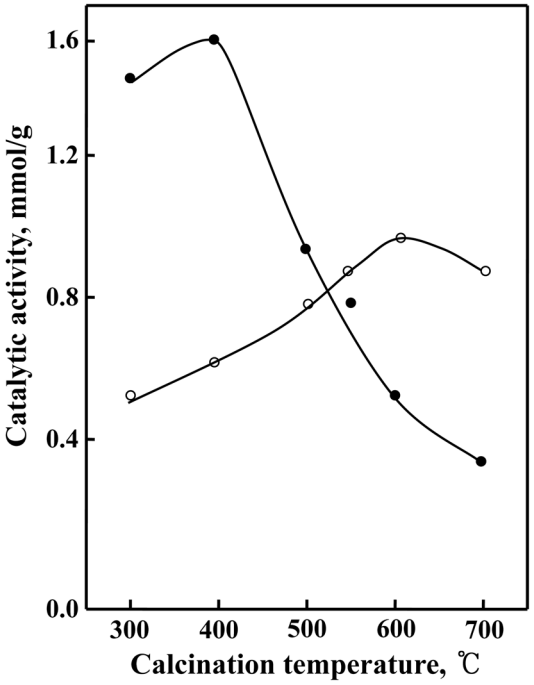

Figure 8. Catalytic activities of 25-NiO/5-La_2O_3-ZrO_2/15-WO_3 for 2-propanol dehydration and cumene dealkylation as a function of calcination temperature: ● , 2-propanol dehydration; ○ , cumene dealkylation.

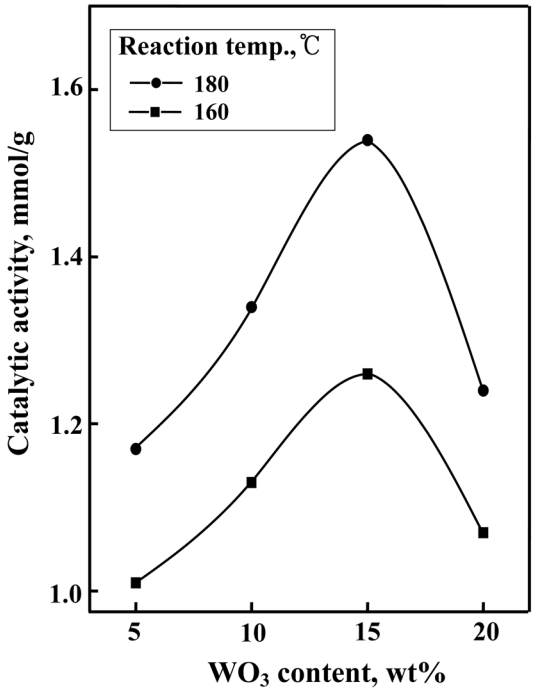

Figure 9. Catalytic activities of 25-NiO/5-La_2O_3-ZrO_2/WO_3 for 2-propanol dehydration as a function of WO_3 content.

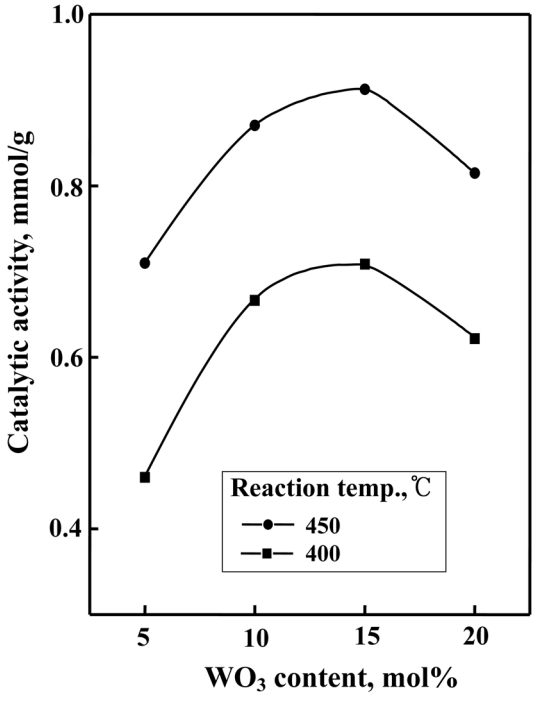

Figure 10. Catalytic activities of 25-NiO/5-La_2O_3-ZrO_2/WO_3 for cumene dealkylation as a function of WO_3 content.

Lewis acid sites,[44-46] indicating the presence of both Brönsted and Lewis acid sites on the surface of 25-NiO/5-La_2O_3-ZrO_2/15-WO_3 sample. Other samples having different WO_3 and NiO contents also showed the presence of both Lewis and Brönsted acids.

Catalytic Activities for Acid Catalysis. Catalytic activities of 25-NiO/5-La_2O_3-ZrO_2/15-WO_3 for both 2-propanol dehydration and cumene dealkylation are plotted as a function of calcination temperature in Figure 8. The activity for 2-propanol dehydration exhibited a maximum at 400 °C, whereas that for cumene dealkylation reached a maximum at 600 °C. This difference between two reactions is due to the fact that the acid strength necessary to two reactions is different each other. Namely, it has been known that 2-propanol dehydration takes place very readily on weak acid sites, while cumene dealkylation does on relatively strong acid sites of catalysts. So, after this, for 2-propanol dehydration emphasis has been placed on the catalysts calcined at 400 °C, while for cumene dealkylation emphasis has been placed on the catalysts calcined at 600 °C.

The catalytic activity of 25-NiO/5-La_2O_3-ZrO_2/WO_3 for the 2-propanol dehydration is measured; the results are illustrated as a function of the WO_3 content in Figure 9, where reaction temperature is 160-180 °C. In view of Table 1 and Figure 9, the variation in the catalytic activity for 2-propanol dehydration can be correlated with the change of its acidity, showing the highest activity and acidity for 25-NiO/5-La_2O_3-ZrO_2/15-WO_3. It has been known that 2-propanol dehydration takes place very readily on weak acid sites.[24,44-46] Good correlations have been found in many cases between the acidity and the catalytic activities of solid acids. For example, the rates of both the catalytic decomposition of cumene and the polymerization of propylene over SiO_2-Al_2O_3 catalysts were found to increase with increasing acid amounts at strengths $H_0 \leq +3.3$.[47] The catalytic activities for both reactions, 2-propanol dehydration

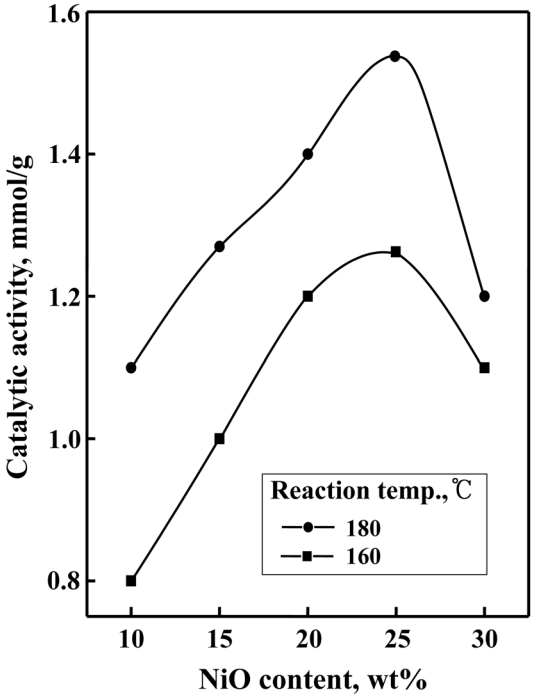

Figure 11. Catalytic activities of NiO/5-La$_2$O$_3$-ZrO$_2$/15-WO$_3$ for 2-propanol dehydration as a function of NiO content.

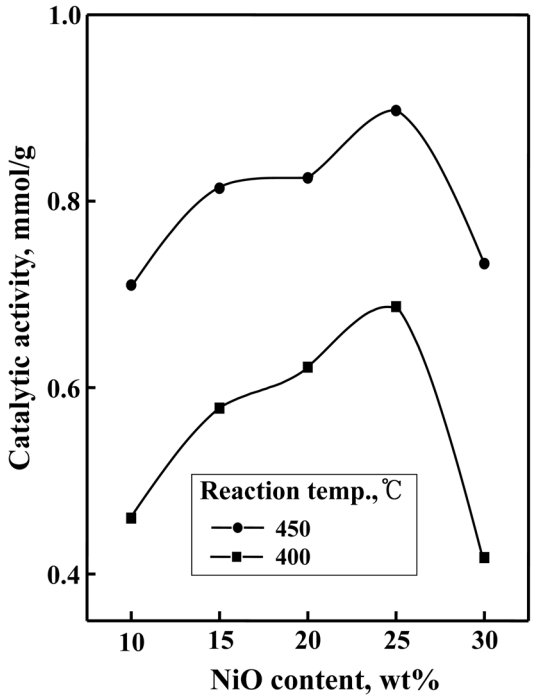

Figure 12. Catalytic activities of NiO/5-La$_2$O$_3$-ZrO$_2$/15-WO$_3$ for cumene dealkylation as a function of NiO content.

and cumene dealkylation, were correlated with the acidity of $NiSO_4$ supported on TiO_2-ZrO_2 measured by an ammonia chemisorption method.[25] It was also reported that the catalytic activity of nickel silicates in the ethylene dimerization as well as in the butene isomerization was closely correlated with the acid amount of the catalyst.[48]

Catalytic activities for cumene dealkylation against the WO_3 content are presented in Figure 10, where reaction temperature is 400-450 °C. The catalytic activities increased with increasing the WO_3 content, reaching a maximum at 15 wt% similar to the results of 2-propanol dehydration in Figure 9. Comparing Table 1 and Figure 10, the catalytic activity is also correlated with the acidity. The correlation between catalytic activity and acidity holds for both reactions, cumene dealkylation and 2-propanol dehydration, although the acid strength required to catalyze acid reaction is different depending on the type of reactions.[24,44-46] As seen in Figures 9 and 10, the catalytic activity for cumene dealkylation, in spite of higher reaction temperature, is lower than that for 2-propanol dehydration. It is also remarkable that the catalysts without WO_3 exhibit no catalytic activities for both 2-propanol dehydration and cumene dealkylation, indicating that WO_3 component plays an important role in the formation of acid sites and the increased catalytic activities for both reactions.

Effect of NiO and La$_2$O$_3$ on Catalytic Activity. The catalytic activities of NiO/5-La$_2$O$_3$-ZrO$_2$/15-WO$_3$ for both 2-propanol dehydration and cumene dealkylation containing different NiO contents were examined; the results are shown as a function of NiO content in Figures 11 and 12, respectively. Catalysts were pretreated at 400 °C for 1h before each

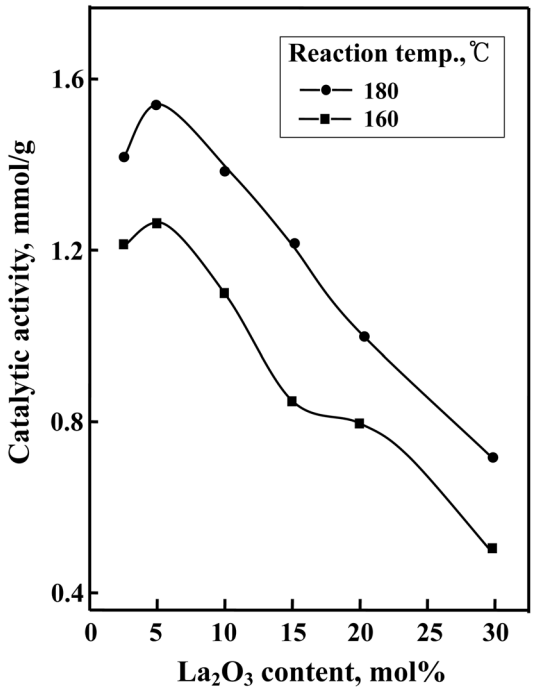

Figure 13. Catalytic activities of 25-NiO/La$_2$O$_3$-ZrO$_2$/15-WO$_3$ for 2-propanol dehydration as a function of La$_2$O$_3$ content.

reaction. The catalytic activities for both reactions increased with increasing the NiO content, reaching a maximum at 25 wt%. Considering the experimental results of Table 2 and Figures 11 and 12, its seems likely that the catalytic activities for both reactions closely relates to the change of the acidity of catalysts. For NiO/5-La$_2$O$_3$-ZrO$_2$/15-WO$_3$ the

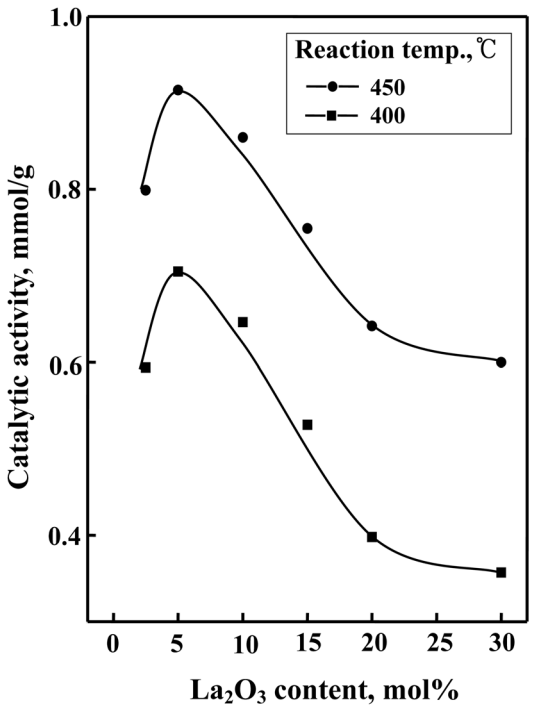

Figure 14. Catalytic activities of 25-NiO/La_2O_3-ZrO_2/15-WO_3 for cumene dealkylation as a function of La_2O_3 content.

catalytic activities and acidity reached maxima at 25 wt% of NiO. The presence of NiO may attract reactants and enhance the local concentration of reactants near the acid sites,[49] consequently showing the increased catalytic activities.

The catalytic activities of 25-NiO/La_2O_3-ZrO_2/15-WO_3 as a function of La_2O_3 content for both reactions was also examined; the results are shown in Figures 13 and 14, respectively. For both reactions the catalytic activities increased with increasing the La_2O_3 content, reaching a maximum at 5 mol%. Considering the experimental results of Table 3 and Figures 13 and 14, the catalytic activities are also related to the changes of the acidity of catalysts. It was reported that a small amount of rare-earth elements in zirconia powder can stabilize the tetragonal and cubic phases over a wide range of temperature.[22] This high surface area of La-doped samples compared with undoped samples is due to the doping effect of La_2O_3 which makes zirconia a stable tetragonal phase as confirmed by XRD.[50,51] The role of La_2O_3 in the catalysts is to form a thermally stable solid solution with zirconia and consequently to give their high surface area and acidity.[22,40]

Conclusions

For NiO/La_2O_3-ZrO_2/WO_3 catalyst, no diffraction line of nickel oxide was observed, indicating good dispersion of nickel oxide on the surface of catalyst. The interaction between tungsten oxide and ZrO_2 increased the acidity and acid strength due to the double bond nature of the W=O in the complex formed on the surface of catalyst. The La_2O_3 formed a solid solution with ZrO_2, giving high surface area and acidity. The high catalytic activities of NiO/La_2O_3-ZrO_2/WO_3 for both 2-propanol dehydration and cumene dealkylation were related to the increase of acidity and thermal stability due to the effects of WO_3 modifying and La_2O_3 doping.

Acknowledgement. We wish to thank Korea Basic Science Institute (Daegu Branch) for the use of X-ray diffractometer.

References

1. Sohn, J. R. *J. Ind. Eng. Chem.* **2004**, *10*, 1.
2. Tanabe, K.; Misono, M.; Ono, Y.; Hattori, H. *New Solid Acids and Bases;* Elsevier Science: Amsterdam, 1989; Chap. 4.
3. Arata, K. *Adv. Catal.* **1990**, *37*, 165.
4. Davis, B. H.; Keogh, R. A.; Srinivasan, R. *Catal. Today* **1994**, *20*, 219.
5. Cheung, T. K.; d'Itri, J. L.; Lange, F. C.; Gates, B. C. *Catal. Lett.* **1995**, *31*, 153.
6. Olag, G. A.; Prakash, G. K. S.; Sommer, J. *Superacids;* Wiley-Interscience: New York, 1985; p 33.
7. Ward, D. A.; Ko, E. I. *J. Catal.* **1994**, *150*, 18.
8. Vaudagna, S. R.; Comelli, R. A.; Canavese, S. A.; Figoli, N. S. *J. Catal.* **1997**, *169*, 389.
9. Kustov, L. M.; Kazansky, V. B.; Figueras, F.; Tichit, D. *J. Catal.* **1994**, *150*, 143.
10. Sayari, A.; Yang, Y.; Song, X. *J. Catal.* **1997**, *167*, 346.
11. Hsu, C. Y.; Heimbuch, C. R.; Armes, C. T.; Gates, B. C. *J. Chem. Soc., Chem. Commun.* **1992**, 1645.
12. Cheung, T. K.; Gates, B. C. *J. Catal.* **1997**, *168*, 522.
13. Adeeva, V.; de Haan, H. W.; Janchen, J.; Lei, G. D.; Schunemann, V.; van de Ven, L. J. M. W.; Sachtler, M. H.; van Santen, R. A. *J. Catal.* **1995**, *151*, 364.
14. Wan, K. T.; Khouw, C. B.; Davis, M. E. *J. Catal.* **1996**, *158*, 311.
15. Song, X.; Reddy, K. R.; Sayari, A. *J. Catal.* **1996**, *161*, 206.
16. Coelho, M. A.; Resasco, D. E.; Sikabwe, E. C.; White, R. L. *Catal. Lett.* **1995**, *32*, 253.
17. Hosoi, T.; Shimadzu, T.; Ito, S.; Baba, S.; Takaoka, H.; Imai, T.; Yokoyama, N. *Prepr. Symp. Div. Petr. Chem.*; American Chemical Society: Los Angeles, CA, 1988; p 562.
18. Ebitani, K.; Konishi, J.; Hattori, H. *J. Catal.* **1991**, *130*, 257.
19. Signoretto, M.; Pinna, F.; Strukul, G.; Chies, P.; Cerrato, G.; Ciero, S. D.; Morterra, C. *J. Catal.* **1997**, *167*, 522.
20. Hino, M.; Arata, K. *J. Chem. Soc. Chem. Commun.* **1987**, 1259.
21. Larsen, G.; Lotero, E.; Parra, R. D. In *Proceedings of the 11th International Congress on Catalysis*; Elsevier: New York, 1996; p 543.
22. Loong , C.-K.; Ozawa, M. *J. Alloys Compd.* **2000**, *60*, 303.
23. Sohn, J. R.; Lee, S. H.; Park, W. C.; Kim, H. W. *Bull. Korean Chem. Soc.* **2004**, *25*, 657.
24. Sohn, J. R.; Seo, D. H.; Lee, S. H. *J. Ind. Eng. Chem.* **2004**, *10*, 309.
25. Sohn, J. R.; Lee, S. H. *Appl. Catal. A: Gen.* **2004**, *266*, 89.
26. Sohn, J. R.; Chun, E. W.; Pae, Y. I. *Bull. Korean Chem. Soc.* **2003**, *24*, 1785.
27. Sohn, J. R.; Cho, S. G.; Pae, Y. I.; Hayashi, S. *J. Catal.* **1996**, *159*, 170.
28. Sohn, J. R.; Park, W. C. *Appl. Catal. A: Gen.* **2002**, *11*, 230.
29. Sohn, J. R.; Han, J. S.; Kim, H. W.; Pae, Y. I. *Bull. Korean Chem. Soc.* **2005**, *26*, 755.
30. Tauster, S. J.; Fung, S. C.; Baker, R. T. K.; Horsley, J. A. *Science* **1981**, *211*, 1121.
31. Wachs, I. E.; Chersich, E. C.; Hardenbergh, J. H. *Appl. Catal.* **1985**, *13*, 335.
32. Sohn, J. R.; Park, M. Y. *Langmuir* **1998**, *14*, 6140.
33. Vuurman, M. A.; Wachs, I. E.; Hirt, A. M. *J. Phys. Chem.* **1991**,

95, 9928.
34. Sohn, J. R.; Kim, J. G.; Kwon, T. D.; Park, E. H. *Langmuir* **2002**, *18*, 1666.
35. Sohn, J. R.; Ryu, S. G. *Langmuir* **1993**, *9*, 126.
36. Mercera, P. D. L.; van Ommen, J. G.; Doesburg, E. B. M.; Burggraaf, A. J.; Ross, J. R. H. *Appl. Catal.* **1990**, *57*, 127.
37. Ebitani, K.; Konishi, J.; Hattori, H. J. *J. Catal.* **1991**, *130*, 257.
38. Adeeva, V.; Lei, G. D.; Sachtler, W. M. H. *Appl. Catal.* **1994**, *118*, L11-L15.
39. Lin, C. H.; Hsu, C. Y. *J. Chem. Soc. Chem. Commun.* **1992**, 1479.
40. Sohn, J. R.; Lim, J. S.; Lee, S. H. *Chem. Lett.* **2004**, *33*, 1490.
41. Roh, H.-S.; Jun, K.-W.; Park, S.-E. *J. Ind. Eng. Chem.* **2003**, *9*, 261.
42. Sohn, J. R.; Park, W. C.; Kim, H. W. *J. Catal.* **2002**, *209*, 69.
43. Sohn, J. R.; Kim, H. W. *J. Mol. Catal.* **1989**, *52*, 361.
44. Sohn, J. R.; Jang, H. J. *J. Mol. Catal.* **1991**, *64*, 349.
45. Decanio, S. J.; Sohn, J. R.; Paul, P. O.; Lunsford, J. H. *J. Catal.* **1986**, *101*, 132.
46. Sohn, J. R.; Han, J. S.; Lim, J. S. *J. Ind. Eng. Chem.* **2004**, *10*, 1003.
47. Tanabe, K. *Solid Acids and Bases;* Kodansha: Tokyo, 1970; p 103.
48. Sohn, J. R.; Ozaki, A. *J. Catal.* **1980**, *61*, 29.
49. Pae, Y. I.; Bae, M. H.; Park, W. C.; Sohn, J. R. *Bull. Korean Chem. Soc.* **2004**, *25*, 1881.
50. Dong, W.-S.; Roh, H.-S.; Jun, K.-W.; Park, S.-E.; Oh, Y.-S. *Appl. Catal. A: Gen.* **2002**, *226*, 63.
51. Roh, H.-S.; Jun, K.-W.; Baek, S.-C. *J. Ind. Eng. Chem.* **2003**, *9*, 168.